

BIBECHANA

ISSN 2091-0762 (Print), 2382-5340 (Online)

Journal homepage: <http://nepjol.info/index.php/BIBECHANA>

Publisher: Department of Physics, Mahendra Morang A.M. Campus, TU, Biratnagar, Nepal

Electronic Structure and Magnetic Properties of Double Perovskites $\text{Ca}_2\text{MnIrO}_6$

Shalika Ram Bhandari^{1,2}, Sarita Lawaju¹, Santosh KC³, Gopi Chandra Kaphle¹ and Madhav Prasad Ghimire^{1*}¹Central Department of Physics, Tribhuvan University, Kirtipur, 44613, Kathmandu, Nepal²Leibniz IFW Dresden, Helmholtzstr. 20, 01069 Dresden, Germany³Chemical and Materials Engineering, San José State University, California, USA

*Email: madhav.ghimire@cdp.tu.edu.np

Article Information:

Received: January 30, 2022

Accepted: February 26, 2022

Keywords:

Density Functional Theory

Double Perovskites

Electronic Structure

Half Metals

Spin-Exchange Coupling

ABSTRACT

Using the density functional theory formalism, electronic and magnetic properties of double perovskites $\text{Ca}_2\text{MnIrO}_6$ are investigated. We found ferrimagnetic ground state with half-metallic nature in $\text{Ca}_2\text{MnIrO}_6$. The electron-correlation, crystal distortion, and spin-orbit coupling (SOC) plays significant role in dictating the electronic properties in this system. From the density of states calculations, a strong hybridization were noted between O-2p, Ir-5d and Mn-3d states resulting $\text{Ca}_2\text{MnIrO}_6$ to half-metal (HM) with metallic state in spin up channel and insulating state in spin-down channel. The HM state persists even when SOC is taken into account, though the spin-polarization reduces slightly. We thus predict $\text{Ca}_2\text{MnIrO}_6$ as a new HM ferrimagnet which can be useful for modern technological applications. We further investigated the Curie temperature of $\text{Ca}_2\text{MnIrO}_6$ by calculating the spin-exchange coupling parameters. Our results are found to be comparable with other perovskites.

DOI: <https://doi.org/10.3126/bibechana.v19i1-2.46404>This work is licensed under the Creative Commons CC BY-NC License. <https://creativecommons.org/licenses/by-nc/4.0/>

1. Introduction

The interest in double perovskite (DPs) with chemical formula $\text{A}_2\text{BB}'\text{O}_6$ (where A = rare earth elements and B & B' = 3d and 4d/5d transition metals (TM)) are increasing due to their novel properties such as crystal field splitting, half-metallicity (HM), ferromagnetism (FM), ferrimagnetism (FiM), Mott-insulating, multiferroicity, etc. [1-8]. These properties are found useful in device fabrication for technological applications. When chemical

substitution is done to the B or B' site, they show additional properties relevant for spintronic devices [9-15]. Among many, HM is one of the important property found in DPs where one spin channel is metallic and the other one is insulating. One such application of HM gives rise to ultra-high density suitable for magnetic recordings. Specifically, DP family containing TM oxides are found to attract researchers because of their unconventional phases [16-18]. For instance, iridate DPs such as $\text{Ln}_2\text{MgIrO}_6$ shows magnetic transition from FM to

AFM state [19,20], magnetic ordering in $\text{La}_2\text{MnIrO}_6$ [21]. Likewise, layered perovskites $\text{Sr}_4\text{Co}_3\text{O}_{10}$ and $\text{Sr}_4\text{Rh}_3\text{O}_{10}$ shows HM-FM state [22] while FiM to HM-FiM and HM-AFM were observed in $\text{Pr}_{2-x}\text{Sr}_x\text{MgIrO}_6$ ($x = 0$ to 2) [23]. Many DPs are reported to have high Curie temperature (T_C) [24-26]. One such example is $\text{Sr}_2\text{CrOsO}_6$ whose T_C is found to be 725 K [27].

In some of the DPs such as Ca_2MWO_6 , Sr_2MWO_6 and Ba_2MReO_6 , where $M = \text{Co}, \text{Ni}$, magnetic atoms at the B/B' sites are 3d/5d and are found to carry opposite spin orientations. This is found to result in octahedral connection exhibiting large crystal distortion [28-30]. Likewise, magnetic phase transition from AFM to FiM takes place when the A-site element Ca was substituted partly by La^{3+} [31].

In this work, we report the electronic, magnetic and exchange coupling in the new yet un-synthesized $\text{Ca}_2\text{MnIrO}_6$. We provide the possibility that the material can be synthesized experimentally and suitable for spintronic applications due to sizable T_C .

Crystal structure and computational details

Figure 1 shows the crystal structure of $\text{Ca}_2\text{MnIrO}_6$ with space group $P21/n$ and its monoclinic structure is maintained by MnO_6 and IrO_6 octahedra. The crystal parameters used for our calculations are $a = 5.351 \text{ \AA}$, $b = 5.456 \text{ \AA}$, $c = 7.620 \text{ \AA}$ and $\beta = 90.092$ [32]. The symmetrized structure of $\text{Ca}_2\text{MnIrO}_6$ with one atom each of Ca, Mn, Ir and three oxygen was transformed to $P1$ space group consisting of 4 Ca, two each of Mn and Ir and 12 oxygen atoms resulting to 20 in-equivalent atoms within a unit cell.

The density functional theory (DFT) calculations is performed using the full-potential linearized augmented plane wave (FLAPW) method as implemented in the WIEN2k code [33]. The standard generalized gradient approximation (GGA) within the parametrization of PBE scheme was used for the exchange-correlation energy [34]. In order to consider the electron-electron correlations in TMs, the Hubbard potential U of 6 eV and 1.5 eV were used for Mn and Ir, respectively [35, 36]. Spin orbit coupling (SOC) is also taken into account to compute the magnetic anisotropy energy (MAE). The atomic sphere radii (R_{MT}) used for elements Ca, Mn, Ir and O, were 2.14, 1.94, 2.01 and 1.64 Bohr respectively. Calculations are done with $8 \times 8 \times 6$ k-mesh with energy and charge convergent criteria set to 10^{-8} Ry and $10^{-5}e$.

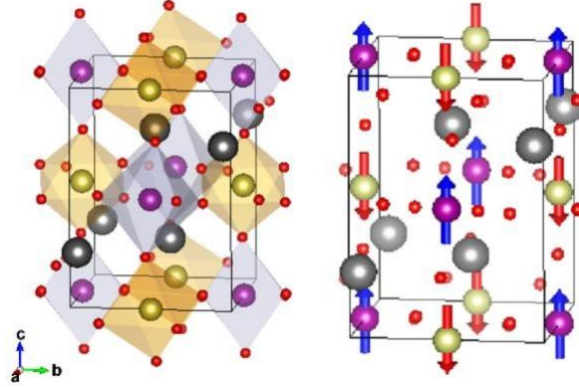


Fig. 1: Crystal structure (left) and ferrimagnetic ground state spin structure (right) of $\text{Ca}_2\text{MnIrO}_6$. The grey, purple, gold and red spheres corresponds to Ca, Mn, Ir and O atoms, respectively.

2. Results and Discussion

We start first by calculating the total energies for the four magnetic configurations (i.e., FM-uuuu, FiM-uudd, AFM1-udud, and AFM2-uddu; where u represents up spin and d represents down spin alignment of magnetic ions). Note that we have two atoms each of Mn and Ir whose magnetic configurations are arranged as Mn1, Mn2, Ir1 and Ir2, respectively. The magnetic arrangement, say FiM-uudd implies the alignment of Mn1-up, Mn2-up, Ir1-down, and Ir2-down spins in FiM configuration. From the above calculation, we found FiM as the magnetic ground state. The discussion below is therefore focused for the FiM configuration of $\text{Ca}_2\text{MnIrO}_6$.

In $\text{Ca}_2\text{MnIrO}_6$, Mn atom carries a charge state +3 with $3d^3$ configuration in which three electrons are distributed in the t_{2g} state in spin up channel and lie in the valence region close to the Fermi level (E_F) while e_g state being empty lies in the conduction region in both spin channel. On the other hand, Ir with charge state +3 and $5d^5$ configuration has five outermost electrons. Due to low-spin state, the five electrons are found to occupy only the t_{2g} states while e_g states being empty lies in the conduction region for both spin channel. As can be seen in the partial DOS of Ir in Fig. 2, the spin-up channel is metallic while spin down remains insulating. This is found consistent with the electron number count of five. This implies that 3 electrons in spin-down channel are fully occupied generating a band gap while two

out of three are occupied in spin up, and thus partially occupied dictating the metallic state.

The spin resolved partial and total DOS of $\text{Ca}_2\text{MnIrO}_6$ within GGA, GGA+ U and GGA+ U +SOC are shown in Fig 2 and Fig 3. The role of partial DOS near E_F (Fig. 2 (a) (left)) are contributed by Mn-3*d*, Ir-5*d* and O-2*p* states. Here, Ir- t_{2g} states are in high spin state as shown in spin down channel while spin up channels are found to be in conduction region. The Ir-5*d* states are found to hybridize strongly with O-2*p* states in the valence region. Due to this hybridization, charge transfer effect was observed where charge is transferred from Ir-5*d* to O-2*p* states giving rise to finite moments in oxygen atoms (see table 1).

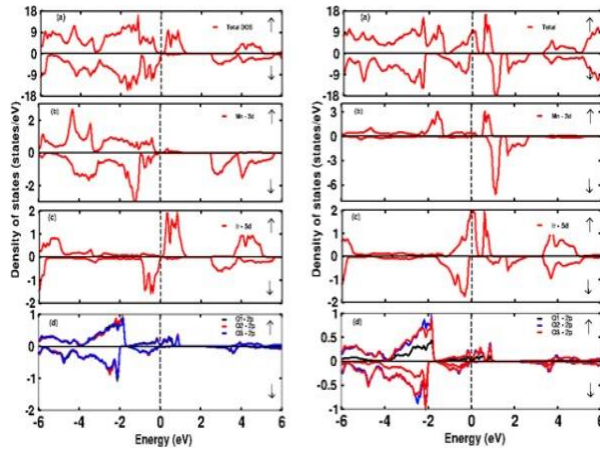


Fig. 2: The DOS of $\text{Ca}_2\text{MnIrO}_6$ within GGA and GGA+ U . The vertical dotted line indicates $E_F = 0$.

The combined effect of electron correlation and SOC is found to generate a pseudo band gap (or a semi-metallic state) in the band structure as shown in Fig. 3 (right). Despite the strong SOC strength of Ir, crystal distortion seems to dominate resulting in the metallic state in spin up channel. SOC effect is found prominent in Ir as it belongs to heavier element. The Ir-5*d* bands splits significantly as shown in Fig 3 which can be well compared with GGA+ U results shown in Fig. 2 (right). Thus, with up spin channel being metallic and down spin channel being insulating, $\text{Ca}_2\text{MnIrO}_6$ shows HM-FiM state which can be confirmed both from DOS and band structure.

Focusing now on magnetic moment within GGA+ U +SOC (see table 1 for details), the individual magnetic moment of Mn, and Ir are calculated to be $3.06 \mu_B$, and $-0.62 \mu_B$ with an

effective magnetic moment of $4.15 \mu_B$ per unit cell in the FiM configurations. This difference in the magnetic moment is due to finite transfer of charges from Mn and Ir to oxygens. As a result, oxygen gain small moment ($\sim 0.06 \mu_B$) and get polarized. The orbital moment of Ir is sizable as compared to Mn while the spin magnetic moment is reduced on Ir because of the Ir-O hybridization.

MAE is also calculated and the obtained value is ~ 9 meV per unit cell with magnetic easy axis along [001] direction (c-axis).

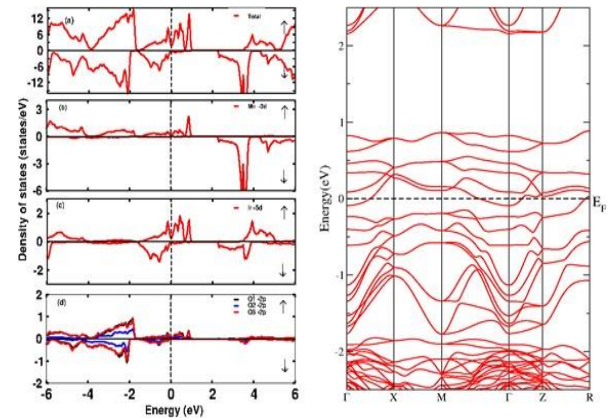


Fig. 3: The DOS and band structures of $\text{Ca}_2\text{MnIrO}_6$ within GGA+ U +SOC.

Table 1: Calculated spin magnetic moments (in μ_B) of Mn, Ir, 3 oxygens and band gap E_g (eV). The calculated orbital moments at Mn and Ir sites are shown within parentheses for $\text{Ca}_2\text{MnIrO}_6$ compound.

Site	GGA	GGA+ U	GA+ U +SOC
Mn	2.84	2.93	3.06/-0.03
Ir	-0.57	-0.61	-0.62/ -0.24
O ₁	-0.05	-0.04	-0.06
O ₂	-0.05	-0.04	-0.06
O ₃	-0.05	-0.04	-0.06
Net	3.25	4	4.15
E_g	Metallic	HM	HM

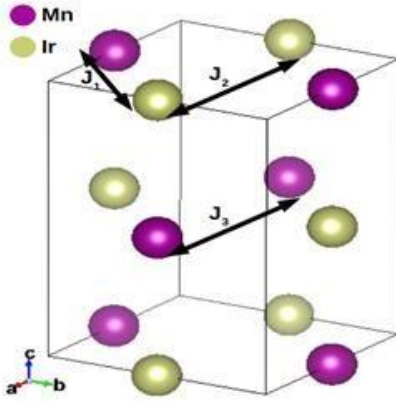


Fig. 4: Magnetic exchange interactions in $\text{Ca}_2\text{MnIrO}_6$.

We also estimated the Curie temperature (T_C) of the material by utilizing the exchange parameters based on the Heisenberg model of the mean-field approximation. The Hamiltonian for the interaction of spins is given by,

$$H = - \sum_{ij} J_{ij} S_i S_j$$

where, J_{ij} is the exchange coupling constant between spins at atomic sites i and j in the crystal, as shown in Fig. 4. S_i and S_j are the spin quantum number at i , and j sub-lattices.

The T_C of the proposed materials using the mean-field theory is given by,

$$T = S S \frac{\sum_{ij} J_{ij}}{3}$$

Using $S_{Mn} = 5/2$ and $S_{Ir} = 3/2$, our calculated T_C is found to be 280 K. The obtained values are found to be in good agreement with the other DPs as reported by Mandal *et al.* [37] and Shalika *et al.* [25].

Conclusions

The electronic and magnetic properties of $\text{Ca}_2\text{MnIrO}_6$ double perovskite has been investigated. $\text{Ca}_2\text{MnIrO}_6$ exhibits ferrimagnetic ground state with magnetic easy axis along [001] direction. The electronic structure calculations incorporating electron-electron correlation and SOC results in half-metallic ferrimagnetic state with up spin channel being metallic and down spin channel as insulating. The metallic states is governed dominantly by Ir-5d orbitals hybridizing with the O-2p states. The magnetic exchange coupling dictates that $\text{Ca}_2\text{MnIrO}_6$ can have large value of T_C

suggesting that this material as a suitable for application in the room-temperature regime.

Acknowledgments

SRB acknowledges Nepal Academy of Science and Technology, Nepal for the PhD fellowship. MPG thanks the AvH Foundation, Germany for equipment grants and IFW-Dresden, Germany for providing equipment for scientific computations to Tribhuvan University. SRB and MPG thanks Manuel Richter for fruitful discussions and Ulrike Nitzsche for the technical assistance.

References

- [1] M.T. Anderson et al; B-cation arrangements in double perovskites, Prog. Solid. State Chem. 22(3) (1993)197-223. [https://doi.org/10.1016/0079-6786\(93\)90004-B](https://doi.org/10.1016/0079-6786(93)90004-B)
- [2] O. Bidault et al; Polaronic relaxation in perovskites, Phys. Rev. B 52(6) (1995) 4191-4197. <https://doi.org/10.1103/PhysRevB.52.4191>
- [3] S. R. Bhandari et al; Electronic, magnetic, optical and thermoelectric properties of $\text{Ca}_2\text{Cr}_{1-x}\text{Ni}_x\text{OsO}_6$ double perovskites, RSC Adv. 10(6) (2020) 16179-16186. <https://doi.org/10.1039/C9RA10775D>
- [4] R. Viana et al; Dielectric spectroscopy in SrTiO_3 , Phys. Rev. B 50(1) (1994) 601-604. <https://doi.org/10.1103/PhysRevB.50.601>
- [5] B. Salce et al; Disorder and thermal transport in undoped KTaO_3 , J. Phys.: Condens. Matter 6(22) (1994) 4077-4092. <https://doi.org/10.1088/0953-8984/6/22/007>
- [6] S. Bhandari et al; First principles investigations on the electronic and magnetic properties of $\text{La}_4\text{Ba}_2\text{Cu}_2\text{O}_{10}$, J. Nep. Phy. Soc. 3(1) (2016) 89-96. <https://doi.org/10.3126/jnphysoc.v3i1.14448>
- [7] A. Sadoc et al; Quantum chemical study of the nature of the ground state and the pressure-induced spin transition in CaFeO_3 , Phys. Rev. B 75(16) (2007) 165116-165123. <https://doi.org/10.1103/PhysRevB.75.165116>
- [8] A. Fert, Nobel lecture: origin, development, and future of spintronics, Rev. Mod. Phys. 80(4) (2008) 1517-1530. <https://doi.org/10.1103/RevModPhys.80.1517>
- [9] S.A. Wolf et al; Spintronics: a spin-based electronics vision for the future, Science 294(5546) (2001) 1488-1495.

- <https://www.science.org/doi/10.1126/science.1065389>
- [10] K.I. Kobayashi et al; Room-temperature magnetoresistance in an oxide material with an ordered double-perovskite structure, *Nature* 395(6703) (1998) 677-680.
<https://doi.org/10.1038/27167>
- [11] D.D. Sarma et al; Electronic structure of $\text{Sr}_2\text{FeMoO}_6$, *Phys. Rev. Lett.* 85(22) (2000) 2549-2552. <https://doi.org/10.1103/PhysRevLett.85.2549>
- [12] Y. Tokura, Critical features of colossal magnetoresistive manganites, *Rep. Prog. Phys.* 69(3) (2006) 797-851.
<https://doi.org/10.1088/0034-4885/69/3/R06>
- [13] Y. Shimakawa et al; Multiferroic compounds with double-perovskite Structures, *Materials* 4(1) (2011) 153-168.
<https://doi.org/10.3390/ma4010153>
- [14] N.S. Rogado et al; Magneto capacitance and magneto resistance near room temperature in a ferromagnetic semiconductor: $\text{La}_2\text{NiMnO}_6$, *Adv. Mater.* 17(18) (2005) 2225-2227.
<https://doi.org/10.1002/adma.200500737>
- [15] B. Mali et al; Re-entrant spin reorientation transition and Griffiths-like phase in antiferromagnetic $\text{TbFe}_{0.5}\text{Cr}_{0.5}\text{O}_3$, *Phys. Rev. B* 102(1) (2020) 014418-014428.
<https://doi.org/10.1103/PhysRevB.102.014418>
- [16] O. Erten et al; Theory of half-metallic double perovskites, II. effective spin Hamiltonian and disorder effects. *Phys. Rev. B* 87(16) (2013) 165105-165112.
<https://doi.org/10.1103/PhysRevB.87.165105>
- [17] H.L. Feng et al; High-temperature ferrimagnetism driven by lattice distortion in double perovskite $\text{Ca}_2\text{FeOsO}_6$, *J. Am. Chem. Soc.* 136(9) (2014) 3326-3329.
<https://doi.org/10.1021/ja411713q>
- [18] H. L. Feng et al; $\text{Ba}_2\text{NiOsO}_6$: A Dirac-mott insulator with ferromagnetism near 100 K, *Phys. Rev. B* 94(23) (2016) 235158-235166.
<https://doi.org/10.1103/PhysRevB.94.235158>
- [19] S.J. Mugavero III et al; Crystal growth, structure and magnetic properties of the double perovskites $\text{Ln}_2\text{MgIrO}_6$ (Ln=Pr, Nd, Sm-Gd), *J. Sol. Stat. Chem.* 183(2), (2010) 465-470.
<https://doi.org/10.1016/J.JSSC.2009.11.025>
- [20] R.A. de Groot et al; New class of materials: half-metallic ferromagnets. *Phys. Rev. Lett.* 50(25) (1983) 2024-2027.
- <https://doi.org/10.1103/PhysRevLett.50.2024>
- [21] P.C. Rout and U. Schwingenschlöggl, Large magneto crystalline anisotropy and giant coercivity in the ferrimagnetic double perovskite $\text{Lu}_2\text{NiIrO}_6$, *Nano Lett.* 21(16) (2021) 6807-6812.
<https://doi.org/10.1021/acs.nanolett.1c01450>
- [22] M.P. Ghimire et al; Half metallic ferromagnetism in tri-layered perovskites $\text{Sr}_4\text{T}_3\text{O}_{10}$ (T = Co, Rh), *J. Appl. Phys.* 117(6) (2015) 063903-063908.
<https://doi.org/10.1063/1.4907933>
- [23] M.P. Ghimire et al; Possible half-metallic antiferromagnetism in an iridium double-perovskite material, *Phys. Rev. B* 93(13) (2016) 134421-134425.
<https://doi.org/10.1103/PhysRevB.93.134421>
- [24] K. -W. Lee & W. E Pickett, Orbital-quenching induced magnetism in $\text{Ba}_2\text{NaOsO}_6$, *EPL* 80(3) (2007) 37008-37013.
<https://doi.org/10.1209/0295-5075/80/37008>
- [25] S.R. Bhandari et al; Electronic structure and estimation of Curie temperature in $\text{Ca}_2\text{B}^{\text{I}}\text{IrO}_6$ (B = Cr, Fe) double perovskites, *J. Appl. Phys.* 130(17) (2021) 173902-173910.
<https://doi.org/10.1063/5.0069884>
- [26] W. Hua, Electronic structure study of double perovskites A_2FeReO_6 (A =Ba, Sr, Ca) and $\text{Sr}_2\text{MM}'\text{O}_6$ (M = Cr, Mn, Fe, Co) by LSDA and LSDA+U, *Phys. Rev. B* 64(12) (2001) 125-126.
<https://doi.org/10.1103/PhysRevB.64.125126>
- [27] Z. Fang et al; Strong ferromagnetism and weak antiferromagnetism in double perovskites: Sr_2FeMO_6 (M = Mo, W, and Re), *Phys. Rev. B* 63(18) (2001) 180407-180411.
<https://doi.org/10.1103/PhysRevB.63.180407>
- [28] A.B. Dutta et al; Magnetic structure of double perovskites Ca_2MWO_6 (M= Co, Ni): A first principles study, *J. Magn. Magn. Mat.* 3(22) (2010) L25-L27.
<https://doi.org/10.1016/j.jmmm.2010.01.019>
- [29] S.Z. Tian et al; Structure and properties of the ordered double perovskites Sr_2MWO_6 (M= Co, Ni) by sol gel route, *Materials Letters* 60(21) (2006) 2747-2750.
<https://doi.org/10.1016/j.matlet.2006.01.083>
- [30] A.W. Sleight & J.F. Weiher, Magnetic and electrical properties of Ba_2MReO_6 ordered perovskites, *J. Phys. Chem. Solids* 33(13) (1972) 679-687.

[https://doi.org/10.1016/0022-3697\(72\)90076-5](https://doi.org/10.1016/0022-3697(72)90076-5)

[31] Bufaceal et al; Physical properties of disordered double-perovskite $\text{Ca}_{2-x}\text{La}_x\text{FeIrO}_6$, J. Appl. Phys. 103 (2008) 07F716.

<https://doi.org/10.1063/1.2830719>

[32] R. Morrow et al; The effect of chemical pressure on the structure and properties of A_2CrOsO_6 (A= Sr, Ca) ferrimagnetic double perovskite, J. Solid Stat. Chem. 238(4) (2016) 46-52.

<https://doi.org/10.1016/j.jssc.2016.02.025>

[33] P. Blaha et al; (2008). An augmented plane wave plus local orbitals program for calculating crystal properties: Wien2K users guide, Techn. Universitat Wien.

<http://susi.theochem.tuwien.ac.at/>

[34] J.P. Perdew, K. Burke, & M. Ernherhof, Generalization gradient approximation made simple, Phy. Rev. Lett. 77(18) (1996) 3865-3868.

<https://doi.org/10.1103/PhysRevLett.77.3865>

[35] P. Hohenberg & W. Kohn., Inhomogeneous electron gas, Phy. Rev. 136(3B) (1964) B864-B871.

<https://doi.org/10.1103/PhysRev.136.B864>

[36] W. Kohn & L.J. Sham, Self-consistent equations including exchange and correlation effects, Phys. Rev. A 140(4A) (1965) A1133-A1138.

<https://doi.org/10.1103/PhysRev.140.A1133>

[37] T.K. Mandal et al; Magnetic and electronic properties of double perovskites and estimation of their Curie temperatures by ab initio calculations, Phys. Rev. B 78(13) (2008) 134431-134440.

<https://doi.org/10.1103/PhysRevB.78.134431>